PRE-ACCRETIONARY AQUEOUS ALTERATION OF DUST IN FINE-GRAINED CHONDRULE RIMS: EVIDENCE FROM PRESOLAR GRAIN ABUNDANCES AND MINERALOGY IN PRIMITIVE CO3.0 CHONDRITES. P. Haenecour[1,2,3], C. Floss[1], T.J. Zega[3], T.K. Croat[1], A. Wang[2], B.L. Jolliff [2], and P. Carpenter[2]. [1]Laboratory for Space Sciences and Physics Dept., [2]Dept. of Earth and Planetary Sciences, Washington University in St. Louis, 1 Brookings Drive, St. Louis, MO 63130, USA. [3]Lunar and Planetary Laboratory, University of Arizona, 1629 E. University Blvd, Tucson, AZ 85721-0092, USA. (pierre@lpl.arizona.edu)

Introduction: Although fine-grained materials in chondrites have been investigated for decades, their origin(s) remain unclear. In particular, the origin of fine-grained chondrule rims (FGRs) in many chondrites, and the possible relationship of these rims to chondrules and/or matrix materials is still uncertain. Several hypotheses have been proposed to explain the formation of FGRs: formation by re-condensation of chondrule volatile elements or disaggregation of chondrule material [1]; formation by dust accretion in the solar nebula before their incorporation into asteroids [2-5]; or formation by impact-related compression of matrix material around chondrules on their parent asteroids [6]. To investigate the origin of FGRs, we compared presolar grain abundances, elemental compositions and mineralogies in individual fine-grained interstitial matrix regions and FGRs in the CO3.0 chondrites ALHA77307 (ALHA), LAP 031117 (LAP) and DOM 08006 (DOM).

Experimental Methods: We searched for presolar grains using NanoSIMS raster ion imaging of $^{12,13}C$ and $^{16,17,18}O$ isotopes in thin sections of the three meteorites. Subsequently, Auger energy spectra and high resolution elemental maps were also acquired for most of the grains using the PHI 700 Auger Nanoprobe. We also acquired X-ray elemental maps and determined the major-element concentrations in several individual matrix areas and FGRs using a JEOL JXA-8200 Superprobe. Several regions of interest were extracted and thinned to electron transparency for detailed mineralogic analysis using the FEI Nova 200 FIB-SEM at ASU and FEI Quanta 3D FIB-SEM at NASA-JSC and Washington University. The FIB sections were then analyzed using

the 200 keV JEOL 2500SE TEM at JSC, the 200 keV JEOL ARM TEM at ASU, and the JEOL 2000FX TEM at Washington University.

Models of FGR Formation in CO3.0 Chondrites: We identified a total of 191 O-anomalous and 35 C-anomalous presolar grains in the matrix regions and FGRs of LAP, ALHA and DOM in the three CO3.0 chondrites. We found presolar grains in all five distinct FGRs that we studied. The identification of presolar grains in FGRs definitively excludes direct formation of the rims from adjacent chondrule material. Moreover, while formation on the parent-body asteroid by impact-related compression cannot be excluded based only on the presence of presolar grains in FGRs, the preservation of presolar grains in the rims is more consistent with a formation via mechanical accretion of dust onto chondrules in the solar nebula. In addition, in ALHA, we identified a unique composite FGR consisting of a small chondrule surrounded by its own distinct rim contained within a larger FGR. The presence of this composite FGR further argues against formation of the FGRs by impact-related compression on the meteorite parent-body, as compression of matrix material on the parent body asteroid should compress fine-grained material (and the small chondrule) into the larger chondrule. Finally, porosity estimates from the EPMA measurements in individual matrix regions and FGRs in LAP and ALHA meteorites showed similarly low porosities (~11 %) between all areas in the two meteorites. This suggests that they experienced similar compaction histories on the parent body asteroids, again inconsistent with a formation of FGRs by impact-related compaction of matrix material.

Lower Presolar Grain Abundances and Localized Aqueous Alteration in FGRs: All three meteorites are characterized by similar overall abundances of O-anomalous (~155 ppm, Fig. 1) and C-anomalous grains (~40 ppm), suggesting that they likely accreted from a nebular reservoir with similar presolar grain abundances. Detailed study of the presolar grain abundances in individual matrix and FGRs also shows systematically lower abundances of O-anomalous grains in the FGRs (average = 67 ± 10 ppm) than in the matrix regions (average = 186 ± 13 ppm) of the three CO3 chondrites., However, the abundances of SiC grains are the same in all areas, within errors (Fig. 1). Because SiC grains are more resistant to secondary processing (e.g., thermal metamorphism and aqueous alteration) than silicate grains [7], the systematic difference in O-anomalous grain abundances observed between the matrices and FGRs likely reflects some type of preferential destruction of presolar silicates by secondary processing in the FGRs without affecting the matrix.

TEM analysis showed that, while matrix areas in LAP are mainly composed of anhydrous Fe-Mg silicate grains in a groundmass of amorphous silicates and nanocrystalline material without significant signs

of aqueous alteration, a FGR (FGR1) shows clear evidence of extensive aqueous alteration with the identification of phyllosilicates mixed with a fine-grained hydrated groundmass throughout the FIB section. These observations are consistent with the presolar silicate abundances, with the more pristine interstitial matrix regions that have significantly higher O-anomalous grains abundance than the aqueously altered FGR. Thus, localized (µm-scale) aqueous alteration in the FGRs appears to be responsible for the destruction (or isotopic re-equilibration) of some presolar silicates in the rims (without affecting the matrix), accounting for the spatial variation of presolar silicate abundances between the matrix and FGRs in CO3.0 chondrites.

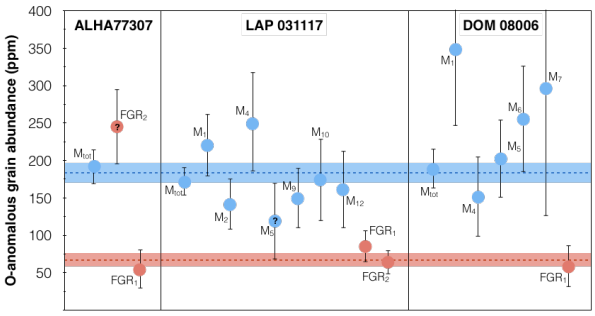

Figure 10. O-anomalous grain abundances in matrix areas (blue dots) and FGRs (red dots) in LAP, DOM and ALHA. The blue and red shaded areas correspond to the average O-anomalous grain abundances in matrix and FGRs, respectively. Errors are 1σ.

Comparison of the Presolar Grain Abundances in FGRs Between CO3 and CR chondrites: Unlike our observations in CO3 chondrites, Leitner et al. [8] reported that the O-anomalous grain abundances are generally higher in FGRs than in the matrix of CR2 chondrites. However, their study also shows that the CR3 chondrite MET 00426 exhibits a similar trend as the CO3.0 chondrites, suggesting a difference between carbonaceous chondrites of petrologic type 3 (most pristine) and type 2 (aqueously altered). While FGRs in both petrologic type 3 and 2 meteorites have similar overall O-anomalous grain abundances within errors (~60-80 ppm), the abundances in the matrix are much lower in type 2 than in type 3 chondrites.

Aqueous alteration on the CR chondrite parent body is believed to be responsible for the lower presolar silicate abundances in the matrix of CR2 than in CR3 chondrites [9]. If this is the case, the difference in O-anomalous grains abundances observed between the matrix and FGRs in type 3 chondrites must reflect other, non-parent body secondary process(es). One possibility is that the low presolar silicate abundances in the FGRs of both CO3 and CR2-3 chondrites is due to aqueous alteration in the solar nebula before their accretion into asteroids. This hypothesis is consistent with a previous model proposed to explain the possible formation of phyllosilicates in FGRs of CM chondrites [2], in which the propagation of shock waves associated with chondrule formation to a water-ice-rich region of the solar nebula beyond the snow line would have induced the vaporization of ice particles and raised the water vapor pressure in this region, allowing the formation of phyllosilicates [2]. In this context, the fine-grained material in FGRs from both CO and CR chondrites could have be affected by similar pre-accretionary aqueous alteration processes. Type 3 CO and CR chondrites were not affected by significant additional secondary processing on their parent body asteroids and, thus, exhibit higher presolar silicate abundances in the interstitial matrix than in the FGRs, while type 2 CR chondrites experienced additional aqueous alteration on their parent body, decreasing the abundances in their matrices to values similar to the abundances in the FGRs. Leitner et al. [8] suggested that FGRs were less affected by parent body aqueous alteration because of their compacted nature.

Conclusions: The ubiquitous presence of presolar silicate grains in FGRs combined with the similar porosity between interstitial matrix regions and FGRs in LAP 031117 and ALHA77307, as well as the identification of a composite FGR in ALHA77307 are all consistent with a formation of FGRs by dust accretion onto freely floating chondrules in the solar nebula before their agglomeration in asteroids.

The identification of localized (µm-sized) aqueous alteration in the FGRs combined with comparison of our data with previous data from CR2 chondrites [8] suggests formation of FGRs in three steps: (1) accretion of dust grains onto freely floating chondrules in the solar nebula, (2) aqueous alteration of the FGRs by melted water ice associated with chondrule-forming shock waves in the solar nebula, and (3) aggregation of FGRs into the CO chondrite parent-body. This model, however, does not preclude the formation of FGRs from different groups of carbonaceous chondrites by different processes, and does not exclude multiple pre-accretionary and/or asteroidal processes for the formation of FGRs in CO3 chondrites.

References: [1] Sears (2011) Cambridge University Press. [2] Ciesla et al. (2003) *Science* 299, 549. [3] Zega & Buseck (2003) *GCA* 67, 1711. [4] Metzler et al. (1992) *GCA* 56, 2873. [5] Bland et al. (2011) *Nat. Geosci.* 4, 244. [6] Trigo-Rodriguez et al. (2006) *GCA* 70, 1271. [7] Floss and Stadermann, (2012) *MAPS* 47, 992. [8] Leitner et al. (2016) *EPSL* 434, 117. [9] Leitner et al. (2012) *ApJ* 745, 38.

Acknowledgment: This work was funded by NASA Earth and Space Science Fellowship NNX12AN77H (P.H.) and NASA Grants NNX14AG25G (C.F.), NNX12AK47G (T.Z.) and NNX13AM22G (A.W.).